BULK COMPOSITIONS OF CAIS AND Al-RICH CHONDRULES: IMPLICATIONS OF THE REVERSAL OF THE ANORTHITE / FORSTERITE CONDENSATION SEQUENCE AT LOW NEBULAR PRESSURES. G. J. MacPherson[1], M. Petaev[2] and A. N. Krot[3]. [1]National Museum of Natural History, Smithsonian Institution, Washington D.C. 20560 USA glenn@volcano.si.edu. [2] Harvard-Smithsonian Center for Astrophysics and Department of Earth and Planetary Sciences, Harvard University, Cambridge MA 02138, USA. [3] Hawai'i Institute of Geophysics and Planetology, University of Hawai'i at Manoa, Honolulu, HI 96822, USA.

Introduction: The bulk compositions of calcium-aluminum-rich inclusions (CAIs) differ slightly but systematically from the predictions of thermodynamic equilibrium for condensation from a hot nebular gas [e.g. 1,2]. The fit is best for melilite-rich (Type A) and hibonite-rich CAIs, but progressively worse for pyroxene-rich (Type B) and, especially, feldspar-rich (Type C) varieties. In essence, Types B and C CAIs are forsterite-deficient relative to predictions. This has led to recent models for Type B CAIs [3, 4] in which melting of condensate precursors is accompanied by distillation of magnesium. Yet even these models do not explain the compositions of plagioclase-rich Type C CAIs. Our recent work on a very different variety of CAI, the so-called fine-grained spinel-rich inclusions (FGIs), has revealed an alternative explanation for the bulk composition problem. FGIs are generally regarded as condensates: most FGIs in the CV3 chondrites are characterized by volatility-fractionated trace element patterns (Group II) that can only have originated through condensation, not evaporation; and, their internal structures are not consistent with igneous crystallization. The best preserved examples (in Efremovka and Leoville) consist of innumerable tiny grains of spinel each wrapped in a succession of thin monomineralic layers of pyroxene and anorthite (e.g. Fig. 1) and, more rarely, melilite. Because FGI bulk compositions closely match those of the igneous Type C CAIs, the FGIs may be the precursors to the Type Cs.

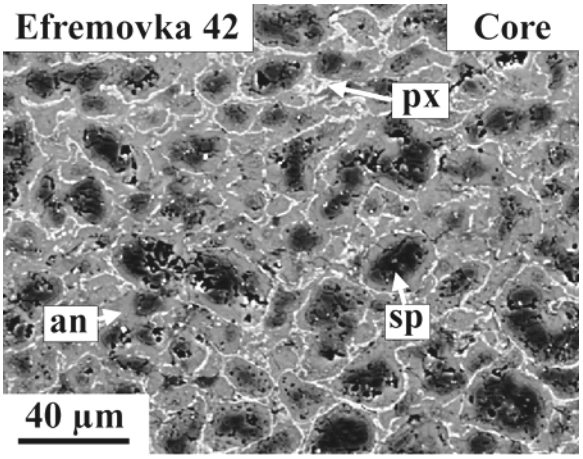

Fig. 1. Back scattered electron photograph of the interior of a fine-grained spinel-rich CAI from Efremovka. Anorthite directly overlies pyroxene, yet canonical condensation calculations predict that forsterite should intervene.

In the context of a condensation model, a critical observation of the FGIs is that even though forsterite is predicted to condense at a higher temperature than anorthite, forsterite is absent from the layered sequence yet anorthite is abundant. This suggests that the forsterite deficiency of CAI bulk compositions may arise prior to any melting, during the condensation stage itself, provided that anorthite precedes forsterite during equilibrium condensation. Petaev and Wood [5] showed that the relative condensation sequence of the two phases is pressure dependent, with lower nebular pressures favoring anorthite to condense prior to (at higher temperatures than) forsterite (Fig. 2).

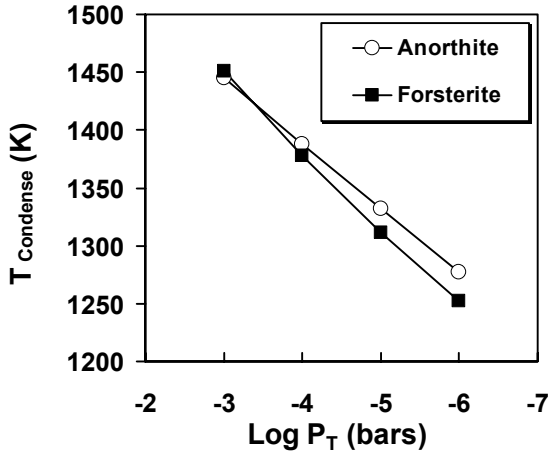

Fig. 2. Calculated condensation (first appearance) temperatures of forsterite and anorthite as a function of total nebular pressure.

We performed full equilibrium thermodynamic condensation calculations at 10^{-3} to 10^{-6} bars total pressure in order to determine the effect on the bulk compositions of total condensed solids.

Results: Fig. 3 shows the calculated condensation trajectories for 10^{-3}, 10^{-5}, and 10^{-6} bars plotted on the ternary diagram corundum (Cor; Al_2O_3) – forsterite (Fo; Mg_2SiO_4) – Ca_2SiO_4 as projected from spinel

($MgAl_2O_4$). Note that the trajectories for the highest-temperature parts of the condensation sequences are not shown, for simplicity; these segments, leading from corundum through hibonite, perovskite, grossite and up to the first appearance of gehlenite (Geh), are essentially the same for the three pressures and do not affect the discussion here. At 10^{-3} bars total pressure (dot-dash line), forsterite begins to condense immediately after calcic pyroxene and the trajectory marches directly in the direction of forsterite, largely missing the field of Types B and C CAIs altogether. In contrast, anorthite precedes forsterite at 10^{-5} bars total pressure (blue dashed line), and as a consequence the trajectory trends toward anorthite and passes directly through the bulk compositions of Types B and C CAIs. Moreover, once forsterite does eventually begin to condense, the trajectory for 10^{-5} bars abruptly turns and passes close to the field of aluminum-rich chondrules. At 10^{-6} bars total pressure (orange dotted line), the first appearance of anorthite is virtually coincident with that of pyroxene and the trajectory misses the Types B and C fields on the forsterite-poor side.

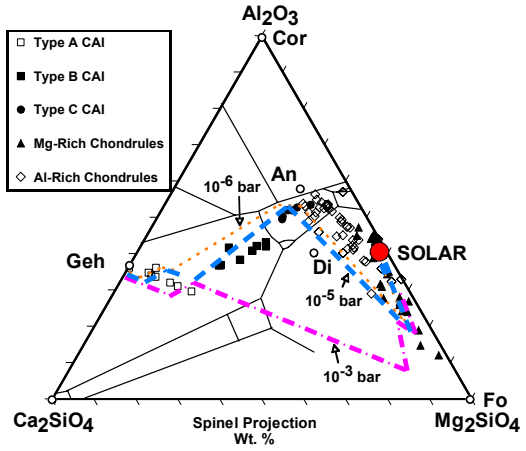

Fig. 3. Calculated bulk composition trajectories for equilibrium condensation at 10^{-3}, 10^{-5}, and 10^{-6} bars total nebular pressure. For details on construction of diagram, see [7].

Discussion: Evidence for small degrees of (heavy) mass-dependent isotopic fractionation in CAIs leaves little doubt that some kind of evaporative process probably did play a role in the evolution of CAI bulk compositions [e.g. 6]. The question is whether it played the dominant role in determining the deviation of the observed bulk composition trend from that predicted by condensation calculations. The model presented herein has several advantages over the models of [3, 4] that attempt to quantify the process of melt evaporation superimposed on condensate precursors as a means of explaining Type B CAI compositions. First, the evaporation model has only been proposed as an explanation for Type B CAIs and does not explain the Type Cs. Also, the FGIs described above have nearly identical forsterite-deficient bulk compositions to the Type Cs but have almost certainly not been melted; thus melt evaporation cannot explain their bulk compositions. It might be argued that Type Cs and FGIs arise from some other mechanism than do other CAIs and hence are unrelated, yet their bulk compositions lie along an extension of the same bulk composition trend defined by the Type Bs. We therefore suggest that they *are* related, and the principal common process they share with other CAIs is condensation under relatively low nebular pressures (~10^{-5} bars). Indeed, early anorthite condensation (caused by a different mechanism) was proposed by [8] as an explanation for the Type C CAIs. Finally, our model suggests how the compositions of aluminum-rich chondrules may relate to those of CAIs and ferromagnesian chondrules, supporting the proposal [8] that aluminum-rich chondrules are intermediate in a volatility sense between CAIs and ferromagnesian chondrules. Condensation at nebular pressures on the order of 10^{-5} bars produces a bulk composition trajectory that passes through the bulk compositions of most CAIs (including Type C) and then close to those of aluminum-rich chondrules as well, finally reaching the composition space occupied by Type I (magnesium-rich) chondrules. It should be noted with respect to aluminum-rich chondrules, however, that this cannot be the entire story. The bulk compositions of most Al-rich chondrules are too silica-rich to be explained by melting of the anorthite- and forsterite-rich condensates; addition of more silica-rich material, e.g., low-Ca pyroxene, is required. Other lines of evidence (incl. oxygen isotopic data) suggest that at least some aluminum-rich chondrules are complex hybrid objects representing multiple isotopic reservoirs [e.g., 10-12]. Nevertheless our model can explain to first order the origin of two of the dominant components of these important objects.

References: [1] Stolper E. (1982) *GCA 46,* 2159-2180; [2] Grossman L. et al. (2000) *GCA 64*, 2879-2894; [3] Grossman L. et al. (2002) *GCA 66*, 145-161; [4] Richter F. M. et al. (2002) *GCA 66*, 521-540; [5] Petaev M. I. and Wood J. A. (1998) *MAPS 33*, A122; [6] Clayton R.N. et al. (1988) *Phil. Trans. R. Soc. Lond. 325,* 483-501; [7] Huss G. et al. (2001) *MAPS 36*, 975-997; [8] Beckett J. R. and Grossman L. (1988) *EPSL 89*, 1-14; [9] MacPherson G. J. and Huss G. R. (2000) *Lunar Planet. Sci. XXXI*, (CD ROM; #1796). [10] Krot A. N. and Keil K. (2002) *MAPS 37*, 91-111; [11] Krot A. N. et al. (2002) *MAPS 37*, 155-182; [12] Krot A. N. (2004) *Lunar Planet. Sci. XXXV*.